09

Enhanced generation efficiency of high-energy multicharged ions under interaction of femtosecond relativistic laser pulses with mixed KrXe clusters

© T.A. Semenov[1], I.M. Mordvincev[2,3], S.A. Shulyapov[2], D.A. Gorlova[2], A.V. Lazarev[4], K.A. Ivanov[2,3], M.S. Dzhidzhoev[2], A.B. Savel'ev[2,3], V.M. Gordienko[2]

[1] Institute of Photon Technologies, Federal Scientific Research Center „Crystallography and Photonics", Russian Academy of Sciences, 142190 Troitsk, Moscow, Russia
[2] Faculty of Physics, Moscow State University, 119991 Moscow, Russia
[3] Lebedev Physical Institute, Russian Academy of Sciences, 119991 Moscow, Russia
[4] Department of Chemistry, Moscow State University, 119991 Moscow, Russia

e-mail: physics.letters@yandex.ru

Received December 10, 2022
Revised January 10, 2023
Accepted January 28, 2023

A new approach is proposed to the production of high-energy ions from a cluster jet irradiated with relativistic ($5 \cdot 10^{18}$ W/cm^2) femtosecond laser pulses, based on the formation of mixed clusters with an Xe core surrounded by a Kr shell. The appearance of distinguished charge states of accelerated ions was registered: instead of low-charge Kr^{2+}, Kr^{3+}, Kr^{4+}, Kr^{5+} for pure Kr clusters, there are three components Kr^{8+}, Kr^{14+}, Kr^{20+} for mixed KrXe clusters. The energy range of detected ions expands significantly: from 1−6 MeV for Kr clusters to 2−16 MeV for KrXe clusters.

Keywords: femtosecond laser pulses, relativistic intensity, ion acceleration, mixed clusters, Kr, Xe.

DOI: 10.61011/EOS.2023.02.55788.12-23

Introduction

Extensive studies have been long ago focused on the production of multicharged high-energy ions during high-intensity laser-matter interaction [1,2]. This is associated with potential wide range of scientific, technology and social applications [3]. Currently, femtosecond laser systems allow to achieve $10^{18}-10^{20}$ W/cm^2 intensity with focusing. Light field strengths meeting these intensities significantly exceed the intraatomic Coulomb field in the hydrogen atom. Emergence of multicharged ions in the cluster nanoplasma is due to the nature of an electric field influencing the atoms and ions and resulting from the action of an external laser field and internal electric fields of the cluster. Moreover, multicharged ions can be formed in a cluster beam with charges exceeding those generated during gas or solid target exposure [4]. It is important that the laser acceleration efficiency for highly charged ions depends on the charge-atomic number ratio Z/A [5]. Charge state of ionized heavy atoms by ultrarelativistic light field may be also used to evaluate the intensity of such emission [6].

Interaction between high-intensity femtosecond laser emission and nanostructured media and, in particular, with clusters is of interest not only for the study of fundamental properties of a substance in extreme nanoplasma generation conditions, but also for various applications [7–9]. Atomic or molecular clusters generated during supersonic expansion of high pressure gas into vacuum hold an intermediate position between gas and condensed state when the average density corresponds to gas and local density corresponds to the liquid or solid phase. They can serve as targets for effective generation of high-energy particles in repetition rate interaction with relativistic-intensity laser emission. Cluster targets are unique due to the ability to achieve considerable absorption of femtosecond laser emission [10]. Essential applications include nuclear fusion reactions [11], generation of high-energy ions [12], electrons [13] and X-ray radiation [14]. The most of studies in the area mentioned above have been performed using homogeneous inert gas clusters. Meanwhile, the experiments based on the generation of laser-induced cluster nanoplasma from binary inert gas clusters are of interest for a number of reasons. Mixed clusters or heteroclusters allow to control X-ray photon output via various channels [15], achieve new nanoplasma generation modes in order to generate neutrons [16].

The change in the cluster composition from initially pure to doped systems and „core−shell" systems allows to control the object structure and charged states of ions and to facilitate charge redistribution inside the cluster

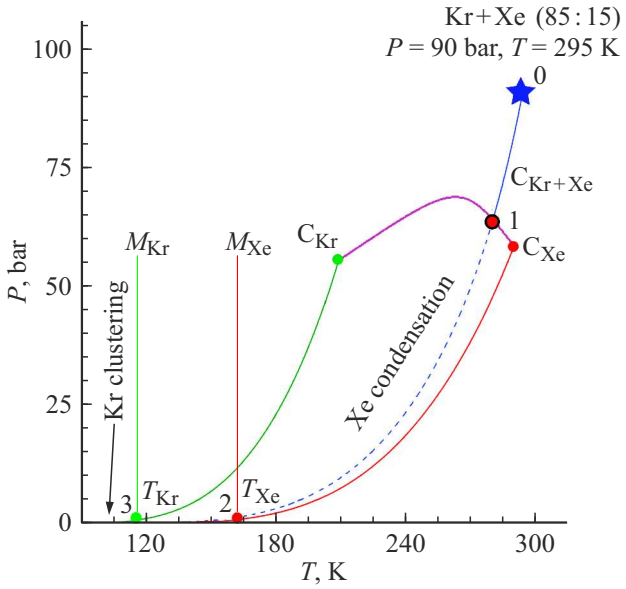

Figure 1. (P, T) diagram of Kr and Xe conditions with Kr:Xe = 0.85:0.15 expansion isentrope from $P_0 = 90$ bar, $T_0 = 298$ K. $C_{Kr}-C_{Xe}$ critical point location line (supercritical locus). M–T, C–T are melting and boiling lines.

leading to Coulomb explosion of outer cluster shell [17]. Mixed clusters containing heavy nucleus Xe and outer shell of Kr can be achieved by means of expansion of a supercritical mixture of krypton with small addition of xenon in a supersonic jet [17]. The purpose of the study is to investigate possible generation of ions with higher ionization multiplicity and almost unchanged maximum energy per unit charge from Kr cluster nanoplasma doped with Xe atoms during exposure to relativistic-intensity femtosecond laser pulses up to $5 \cdot 10^{18}$ W/cm^2.

1. Dynamics of formation, composition and structure of clusters from a mixture of Kr and Xe

The supercritical initial conditions were selected in order to achieve high concentration of clusters in the jet due to density fluctuations in Xe critical transition region. Generation dynamics, composition and structure of clusters formed in supersonic jets of Kr and Xe gas mixture expanding from supercritical conditions will be briefly described below. Behavior of krypton gas with small xenon addition in gasdynamic jets may be tracked by isentrope expansion on (P, T)-diagram of the mixture condition (Figure 1). Figure 1 shows Kr and Xe equilibrium curves and hypothetical isentrope (0–3) of expansion from supercritical initial conditions $P_0 = 90$ bar and $T_0 = 298$ K for Kr : Xe = 0.85 : 0.15 mixture, and critical curve $C_{Kr} - C_{Xe}$. Hypothetical curves were calculated using a simple mixing rule taking into account molar contributions of individual components without taking into account cross terms.

Expansion of initial Kr:Xe=0.85:0.15 mixture at rather high initial pressure $P_0 = 90$ bar at 0 – 1 isentrope section up to the vicinity of critical point C_{Kr-Xe} probably results in formation of primarily dimers and to a minor extent of trimers of Kr and Xe atoms. When the isentrope intersects the critical curve, Xe density fluctuations are growing resulting in fast growth of its clusters against the expanding Kr with small additions of dimers and trimers. In this case, collisions of growing Xe_n clusters with Kr may result in formation of Xe_nKr type mixed clusters, which lose Kr during next collision with Xe atom. This is due to release of energy during collision which is equal to Van der Waals bond energy of Xe–Xe and exceeding the bond energy for Xe–Kr. This „clarification“ from Kr will continue until the growth of Xe clusters stops. After this, nothing prevents the growth of krypton shell [18,19]. The degree of coverage of xenon cluster core with krypton shell will now depend only on the collision rate of the resulting mixed cluster with the krypton component which is, in turn, defined by local density and temperature of Kr. During gas dynamic expansion of the jet in vacuum using a conical nozzle, fast and considerable decrease of density (by orders) and temperature (by times) tales place. This results in fast decrease, mainly due to density decrease, in collision rate, which ensures stop of cluster growth already within the nozzle. Finally, in the recorded region outside the nozzle, nanoparticles formed during expansion shall, as concluded in [19], constitute mixed clusters with Xe core surrounded with Kr shell. As a result of nonlinear interactions between high-intensity radiation and plasma [1], high-energy and highly charged plasma is formed in the xenon core. High-energy photons and fast electrons knock out electrons from xenon plasma from K level of krypton existing in the outer shell. This leads to explosive expansion of the plasma channel with highly charged Kr ions on its front [20]. This phenomenological description correlates with the charge redistribution model leading to the Coulomb explosion of the outer cluster portion and nanoplasma core recombination [17].

2. Experimental setup

2.1. Cluster jet formation and monitoring

Cluster jets were formed during supersonic gas expansion from the conical nozzle into vacuum. Conical nozzle (half-cone angle 5°, throat diameter 0.5 mm, length 10 mm) was joined with the pulse gas valve with an exit of 0.5 mm. Valve opening time was 1 ms. Initial conditions $P_0 = 90$ bar and $T_0 = 298$ K were maintained continuously. Cluster distribution in the jet was measured by the probe laser beam scattering signal [21]. Blue diode laser (445 nm) was used as a probe emission source. Cluster jet width of pure Kr has been found to be ~ 1.7 times greater than for mixed clusters formed from Kr+Xe (85:15) mixture (Figure 2, *a*). This serves to confirm a previous assumption on formation of heavy clusters when Kr+Xe (85:15) mixture is used

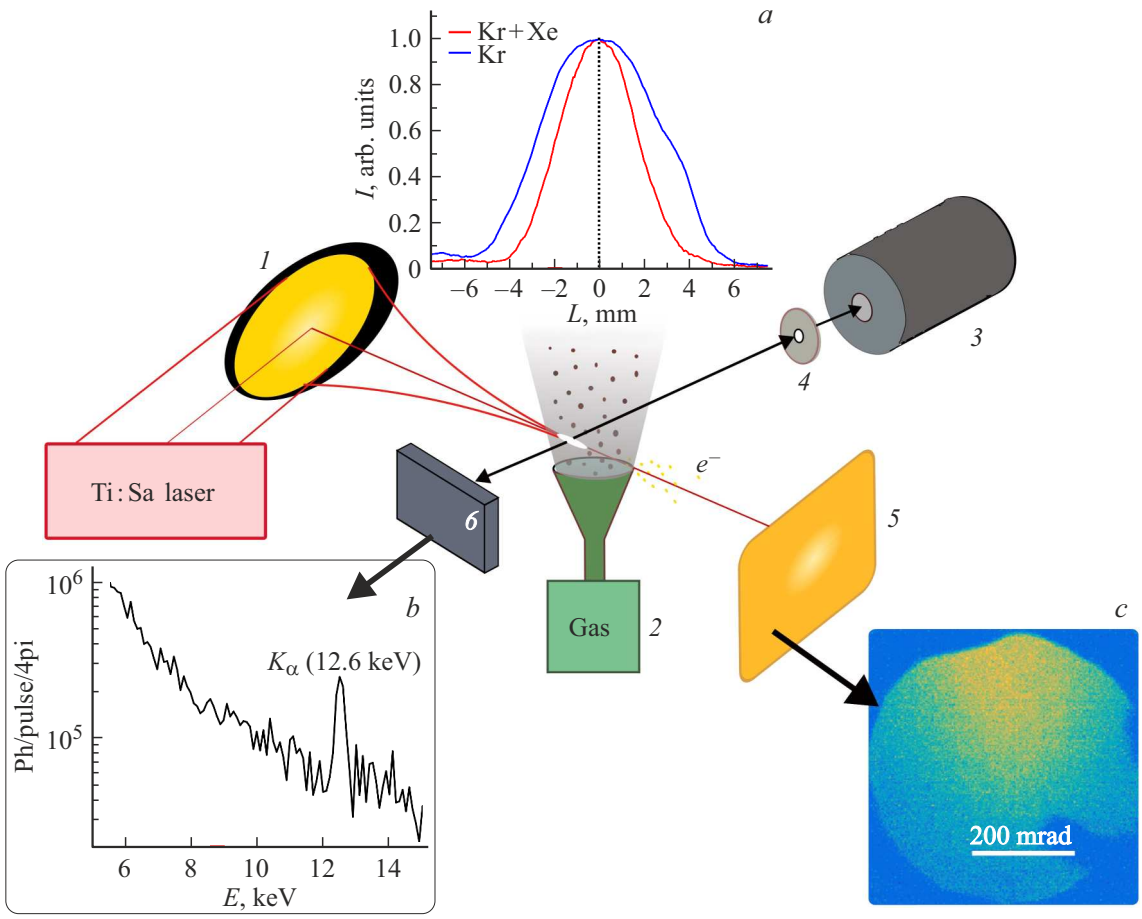

Figure 2. Diagram of the experimental setup for cluster jet exposure to relativistic femtosecond laser pulses: off-axis parabolic mirror (*1*), pulse gas valve with conical nozzle (*2*), Thomson mass-spectrometer (*3*) with diaphragm (*4*), Lanex scintillator (*5*), Greateyes X-ray matrix (*6*). (*a*) scattering signal distribution across the cluster jet 6 mm from the nozzle edge for Kr+Xe and Kr, respectively, (*b*) X-ray spectrum of KrXe nanocluster nanoplasma glow, (*c*) electron beam on Lanex scintillator.

as opposed to Kr, which results in „reduction“ of the jet section [22]. Estimation of the average diameter of mixed KrXe (85:15) clusters on the basis of modified Hagen equations [19] gives a cluster diameter of $d \sim 150$ nm. For similar conditions, the use of pure Kr provides clusters with a diameter of 90 nm [21].

2.2. Materials and experimental technique

High-energy ion experiments were carried out using 0.8 TW Ti:Sa laser emission (pulse energy, width and repetition rate are 40 mJ, 50 fs and 10 Hz, respectively). Amplified spontaneous emission (ASE) contrast was $\approx 10^8$ per 100 ps before the main pulse. Peak intensity $5 \cdot 10^{18}$ W/cm^2 was achieved by means of emission focusing using the off-axis parabolic mirror with $F/D = 5$. The experimental setup diagram is shown in Figure 2. For the purpose of the experiment, the relativistic level of laser intensity was confirmed by recording accelerated electron beams with energy higher than 400 keV on Kodak LANEX scintillator [13]. The accelerated ion spectrum was studied using Thomson mass-spectrometer installed at 135° to the laser beam propagation direction. It is described in detail in [23]. In order to assess the interaction between the laser emission and clusters, X-ray glow of plasma was additionally recorded using Greateyes energy-calibrated silicon-matrix detector (recording range 5–25 keV).

3. Multicharged high-energy ion formation

Ion acceleration from clusters depends to a great extent on the nanoplasma charge. For „heavy“ atom clusters, highly charged ($Z > +10$) states in nanoplasma may be obtained at a laser intensity of $I > 10^{18}$ W/cm^2 [7]. Interaction was optimized by laser focus re-positioning within Kr and KrXe cluster jets with simultaneous recording of the integral output of X-ray radiation and accelerated electron beams. It was found that, when laser emission was focused on the jet edge, the X-ray output was almost unchanged when the distance from the nozzle exit changed in the range from 1mm to 6mm. The presence of Kr in the clusters in mixture with Xe is confirmed by recording

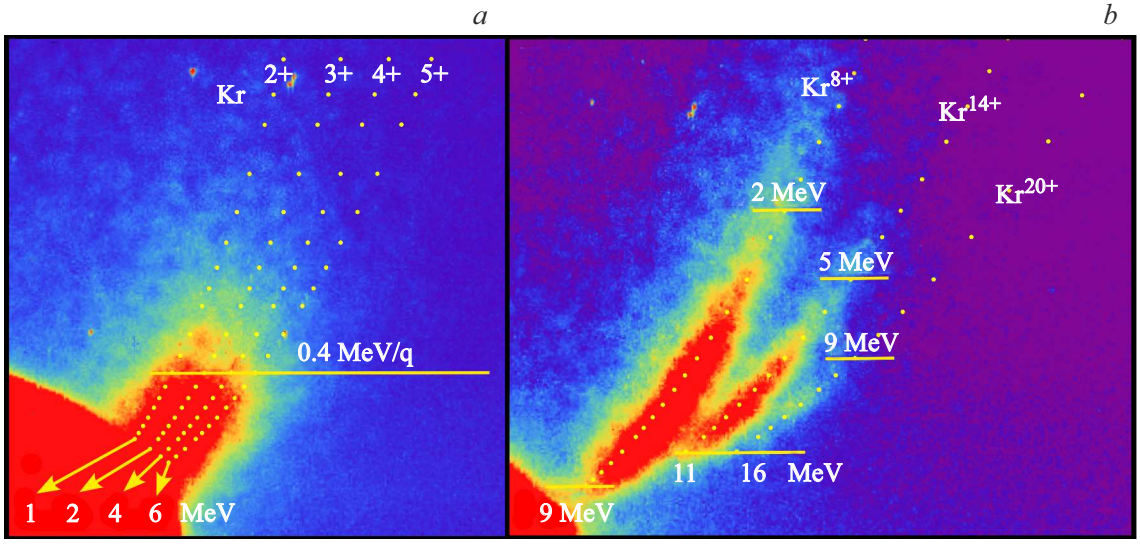

Figure 3. Ion signal in Thomson mass-spectrometer for pure Kr (a) clusters and mixed KrXe (b) clusters.

Kα(12.6 keV) line of Kr in the X-ray glow of nanoplasma (Figure 2, b). At the same time electron acceleration in filamentation mode is observed only in case of focusing at 4−5.5 mm from the nozzle exit and at 2.5−3.5 mm from the nozzle axis (Figure 2, c). Probably, the plasma density at the nozzle exit at the initial pressure of $P_0 = 90$ bar was so high that electrons can not gain the energy before the laser beam collapse. Thus, the X-ray output and electron acceleration data was used to determine the jet region for laser exposure — distance from the nozzle exit was in the range from 4mm to 5.5 mm and the best emission focus position could move at 2.5−3.5 mm from the jet axis.

Magnetic and electric fields in Thomson spectrometer were set such as the recording range was $\sim 0.3-1.8$ MeV/q (energy per charge). The following processing of experimental data made it possible measure accelerated ion charges with an error of ± 1. Figure 3 shows the ion signals for Kr and KrXe clusters. In both cases, the maximum ion energy was equal to $1-1.5$ MeV/q. When pure Kr clusters were used, low charged Kr^{2+}, Kr^{3+}, Kr^{4+}, Kr^{5+} ions with energies from 1 MeV to 6 MeV were recorded. It is known that charges up to 26+ [7] may form in Kr cluster nanoplasma at $I \sim 5 \cdot 10^{18}$ W/cm^2. We have recorded only low charged Kr ions with MeV energy levels. During hydrodynamic expansion of Kr cluster, ion recombination probably takes place resulting to decrease of the observed charges.

When using KrXe (85:15) mixture, the ion signal changes significantly (Figure 3). Thomson mass-spectrometer is not able to distinguish ion species, but rather determines the ratio of ion charge Z to ion mass M. For equal ratio $Z_{Kr}/M_{Kr} = Z_{Xe}/M_{Xe}$, Xe ion charge shall be by 1.57 times higher than for Kr. It should be added that ion charge on the krypton layer of the cluster shall be 1.7 times higher than in Xe core according to the design data on the radial charge distribution heterogeneity in nanoplasma [7]. Therefore, recording of only Kr ions is the more probable scenario for KrXe. As a result of irradiation of mixed KrXe clusters, only parabola corresponding to Kr^{8+}, Kr^{14+}, Kr^{20+} ions are observed. Ion energies were within $2-9$ MeV for Kr^{8+}, $5-11$ MeV for Kr^{14+} and $9-16$ MeV for Kr^{20+}.

According to the findings of [17], it may be expected that charge redistribution takes place in nanoplasma during mixed XeKr cluster exposure to high-intense femtosecond laser emission. Hot nanoplasma electrons leave the cluster causing formation of excessive positive charge in Xe core. The remaining electrons in the cluster will be attracted to the core to compensate the charge disbalance. Xe core in such configuration plays a role of electron collector. This provides conditions for formation of highly charged Kr ions on the shell with following effective acceleration due to the Coulomb repulsion forces. Acceleration mechanism of the selected charge states is probably associated with the features of the effect of Coulomb forces on the mixed KrXe cluster shell and requires further theoretical study.

Thus, transition from pure Kr clusters to mixed KrXe clusters allowed to increase the maximum laser acceleration efficiency of heavy ions from 70 keV/u to 190 keV/u (energy per nucleon) with considerable charge growth (Z/A) from 0.06 q/u to 0.24 q/u.

Conclusion

A new approach was proposed in order to achieve high-energy multicharged ions using mixed Kr+Xe clusters with Xe core surrounded by Kr shell during exposure to relativistic ($5 \cdot 10^{18}$ W/cm^2) femtosecond laser pulses.

Experiments for production of high-energy ions by interaction between femtosecond (50 fs) relativistic ($5 \cdot 10^{18}$ W/cm^2) laser pulses and mixed KrXe clusters formed from single-phase supercritical Kr+Xe mixture

(85:15, $P_0 = 90$ bar and $T_0 = 298$ K) were performed for the first time.

Increase in the charge and energy of accelerated Kr ions was found for mixed KrXe clusters compared with pure Kr clusters. Emergence of selected charge states of accelerated ions was recorded: instead of low-charged Kr^{2+}, Kr^{3+}, Kr^{4+}, Kr^{5+} for Kr clusters, three Kr^{8+}, Kr^{14+}, Kr^{20+} components for KrXe clusters. Recorded ion energy range is expanded considerably: from 1−6 MeV for Kr clusters to 2−16 MeV for mixed KrXe clusters.

Funding

The study was carried out with financial support of RFBR and „Rosatom" State Corporation (project № 20-21-00030 for diagnostics of cluster nanoplasma ion composition). Nanoparticle jet formation methods were developed within the State Assignment of RAS FSRC „Crystallography and Photonics" of the Ministry of Science and Higher Education of the Russian Federation. X-ray glow of nanoplasma was measured using the equipment purchased within „Science" project as of May 20 2020 № AM/6-pr.

Conflict of interest

The authors declare that they have no conflict of interest.

References

[1] M. Roth, M. Allen, P. Audebert, A. Blazevic, E. Brambrink, T.E. Cowan, J. Fuchs, J-C. Gauthier, M. Geißel, M. Hegelich, S. Karsch, J. Meyer-ter-Vehn, H. Ruhl, T. Schlegel, R.B. Stephens. Plasma Phys. Control. Fusion, **44**, B99(2002). DOI: 10.1088/0741-3335/44/12B/308

[2] V.M. Gordienko, I.M. Lachko, A.A. Rusanov, A.B. Savel'ev, D.S. Uryupina, R.V. Volkov. Appl. Phys. B, **80**, 733 (2005). DOI: 10.1007/s00340-005-1781-x

[3] M. Passoni, F.M. Arioli, L. Cialfi, D. Dellasega, L. Fedeli, A. Formenti, A.C. Giovannelli, A. Maffini, F. Mirani, A. Pazzaglia, A. Tentori, D. Vavassori, M. Zavelani-Rossi, V. Russo. Plasma Phys. Control. Fusion, **62** (1), 014022 (2020). DOI: 10.1088/1361-6587/ab56c9

[4] M.B. Smirnov. JETP, **126** (6), 859 (2018). DOI: 10.1134/S1063776118060080.

[5] J. Domański, J. Badziak. Plasma Phys. Control. Fusion, **64**, 085002 (2022). DOI: 10.1088/1361-6587/ac77b6

[6] M.F. Ciappina, S.V. Popruzhenko, S.V. Bulanov, T. Ditmire, G. Korn, S. Weber. Phys. Rev. A, **99** (4), 043405 (2019). DOI: 10.1103/PhysRevA.99.043405

[7] V.P. Krainov, B.M. Smirnov, M.B. Smirnov. Phys. Usp., **50**, 9 (2007). DOI: 10.1070/PU2007v050n09ABEH006287.

[8] K. Ueda et al. J. Phys. B, **52**, 171001 (2019). DOI: 10.1088/1361-6455/ab26d7

[9] S.G. Bochkarev, A. Faenov, T. Pikuz, A.V. Brantov, V.F. Kovalev, I. Skobelev, S. Pikuz, R. Kodama, K.I. Popov, V.Yu. Bychenkov. Sci.Rep., **8**, 9404 (2018). DOI: 10.1038/s41598-018-27665-x

[10] T. Ditmire, R.A. Smith, J.W.G. Tisch, M.H.R. Hutchinson. Phys. Rev. Lett., **78**, 3121 (1997). DOI: 10.1103/PhysRevLett.78.3121

[11] H.J. Quevedo, G. Zhang, A. Bonasera, M. Donovan, G. Dyer, E. Gaul, G.L. Guardo, M. Gulino, M. LaCognata, D. Lattuada, S. Palmerini, R.G. Pizzone, S. Romano, H. Smith, O. Trippella, A. Anzalone, C. Spitaleri, T. Ditmire. Phys.Lett. A, **382** (2−3), 94 (2018). DOI: 10.1016/j.physleta.2017.11.002

[12] M. Kanasaki, S. Jinno, H. Sakaki, A.Ya.Faenov, T.A.Pikuz, M. Nishiuchi, H. Kiriyama, M. Kando, A. Sugiyama, K. Kondo, R. Matsui, Y. Kishimoto, K. Morishima, Y. Watanabe, C. Scullion, A.G. Smyth, A. Alejo, D. Doria, S. Kar, M. Borghesi, K. Oda, T. Yamauchi, Y. Fukuda. Radiation Measurements, **83**, 12 (2015). DOI: 10.1016/j.radmeas.2015.06.011

[13] I.A. Zhvaniya, K.A. Ivanov, T.A. Semenov, M.S. Dzhidzhoev, R.V. Volkov, I.N. Tsymbalov, A.B. Savel'ev, V.M. Gordienko. Laser Phys. Lett., **16**, 115401 (2019). DOI: 10.1088/1612-202X/ab404b

[14] T.A. Semenov, K.A. Ivanov, A.V. Lazarev, I.N. Tsymbalov, R.V. Volkov, I.A. Zhvaniya, M.S. Dzhidzhoev, A.B. Savel'ev, V.M. Gordienko. Quant. Electron., **51** (9), 838 (2021). DOI: 10.1070/QEL17602.

[15] I.A. Zhvaniya, M.S. Dzhidzhoev, V.M. Gordienko. Laser Phys. Lett., **14** (9), 096001 (2017). DOI: 10.1088/1612-202X/aa7d64

[16] A. Heidenreich, J. Jortner, I. Last. PNAS, **103** (28), 10589 (2006). DOI: 10.1073/pnas.0508622103

[17] M. Hoener, C. Bostedt, H. Thomas, L. Landt, E. Eremina, H. Wabnitz, T. Laarmann, R. Treusch, A.R.B. de Castro, T. Möller. J. Phys. B, **41**, 181001 (2008). DOI: 10.1088/0953-4075/41/18/181001

[18] M. Nagasaka, N. Kosugi, E. Rühl. J. Chem. Phys. **136**, 234312 (2012). DOI: 10.1063/1.4729534

[19] O.P. Konotop, S.I. Kovalenko, O.G. Danylchenko, V.N. Samovarov. J. Clust. Sci., **26**, 863 (2015). DOI: 10.1007/s10876-014-0773-6

[20] E. Ackad, N. Bigaouette, S. Mack, K. Popov, L.Ramunno. New J. Phys., **15**, 053047 (2013). DOI: 10.1088/1367-2630/15/5/053047

[21] A.V. Lazarev, T.A. Semenov, E.D. Belega, V.M. Gordienko. J. Supercrit. Fluids, **187**, 105631 (2022). DOI: 10.1016/j.supflu.2022.105631

[22] A.V. Lazarev, K.A. Tatarenko, A.Yu. Amerik. Phys. Fluids, **29**, 087101 (2017). DOI: 10.1063/1.4996584

[23] I.M. Mordvintsev, S.A. Shulyapov, A.B. Savel'ev. Instrum. Exp. Tech., **62** (6), 737 (2019). DOI: 10.1134/S0020441219050208

Translated by E.Ilyinskaya